
SYMBOLIC REGRESSION VIA MDLFORMER-GUIDED SEARCH: FROM MINIMIZING PREDICTION ERROR TO MINIMIZING DESCRIPTION LENGTH

Zihan Yu

Department of Electronic Engineering, BNRist
Tsinghua University
Beijing, China
yuzh23@mails.tsinghua.edu.cn

Jingtao Ding

Department of Electronic Engineering, BNRist
Tsinghua University
Beijing, China
dingjt15@tsinghua.org.cn

Yong Li

Department of Electronic Engineering, BNRist
Tsinghua University
Beijing, China
liyong07@tsinghua.edu.cn

ABSTRACT

Symbolic regression, a task discovering the formula best fitting the given data, is typically based on the heuristical search. These methods usually update candidate formulas to obtain new ones with lower prediction errors iteratively. However, since formulas with similar function shapes may have completely different symbolic forms, the prediction error does not decrease monotonously as the search approaches the target formula, causing the low recovery rate of existing methods. To solve this problem, we propose a novel search objective based on the minimum description length, which reflects the distance from the target and decreases monotonically as the search approaches the correct form of the target formula. To estimate the minimum description length of any input data, we design a neural network, MDLformer, which enables robust and scalable estimation through large-scale training. With the MDLformer’s output as the search objective, we implement a symbolic regression method, SR4MDL, that can effectively recover the correct mathematical form of the formula. Extensive experiments illustrate its excellent performance in recovering formulas from data. Our method successfully recovers around 50 formulas across two benchmark datasets comprising 133 problems, outperforming state-of-the-art methods by 43.92%.

Keywords Symbolic Regression · Minimum Description Length · Transformer · Neural Network Guided Search

1 Introduction

Symbolic regression (SR) is a task that uncovers interpretable mathematical formulas to describe the underlying relationships within observational data, which is widely used for promoting scientific discovery or facilitating the modeling of diverse phenomena in many fields, such as dynamical systems (Quade et al., 2016; Chen et al., 2019; Cornelio et al., 2023; Angelis et al., 2023), materials science (Wang et al., 2019; Schmelzer et al., 2020; Weng et al., 2020; Sun et al., 2019), etc. (Liu et al., 2024; Neumann et al., 2020). Formally, SR aims at finding a symbolic function f from the given data (x, y) , where $x = [x_1, x_2, \dots, x_D] \in \mathbb{R}^{N \times D}$ and $y \in \mathbb{R}^{N \times 1}$ are observed N samples points of independent and dependent variables. The discovered formulas consist of mathematical symbols like $+$, $-$, \times , and \div , whose specific form can provide corresponding insights into the patterns behind the data. To find the formula that best fits the data in the symbolic space, the most typical methods to SR are based on heuristic search, in particular, the genetic programming (GP) algorithm (Augusto & Barbosa, 2000), which executes evolution iteratively to enhance the fit of candidate formulas to the given data. There is now a large body of commercial and open-source software

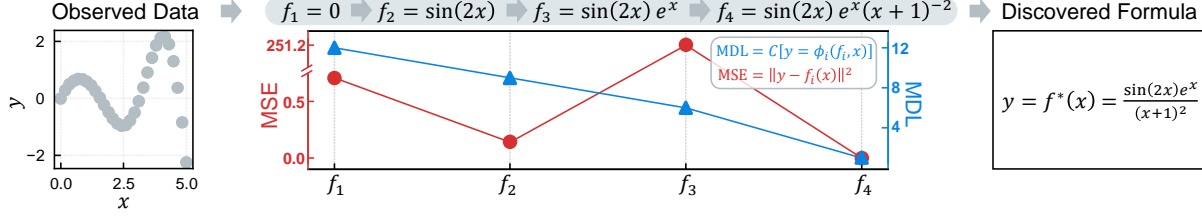


Figure 1: **Comparison of the two search objectives.** In the searching route leading to the target, f^* , the prediction error (measured by the mean square error, MSE) does not decrease monotonically as the candidate formula’s form gets closer to the target one, whereas the minimum description length (MDL) does. Here, ϕ_i denotes the function $f^* = \phi_i(x, f_i)$ and $C[\phi_i]$ is its complexity.

(Dubčáková, 2011; Stephens, 2016; Cranmer, 2023), as well as many influential works (Schmelzer et al., 2020; Weng et al., 2020; Liu et al., 2024), that developed based on the heuristic search-based SR methods.

However, while existing SR methods can identify formulas with high accuracy ($R^2 > 0.99$ for over 90% of cases in SRbench (Cavalab, 2022)), their effectiveness in discovering the optimal formula with the lowest prediction error is limited (only around 20% success rate), even in noise-free data. This is because these methods optimize the candidate formulas’ prediction errors (Makke & Chawla, 2024), which does not lead to the target formula with the minimum prediction error. As illustrated in Figure 1, the mean squared error of a candidate formula (f_i) does not decrease monotonically when its form approaches the target one. This is because formulas with similar symbolic structures can exhibit rather different functional shapes in the numerical space. On the other hand, two formulas with similar functional shapes can have entirely different symbolic forms. This indicates that the SR task lacks an *optimal substructure* (Cormen et al., 2022), that is, the target formula with the minimum prediction error cannot be achieved by simply making small adjustments to formulas with sub-optimal prediction errors. This high nonlinearity of the relationship between a formula’s mathematical form and its functional shape results in a divergence between the direction of reducing prediction error and the direction toward the target formula. This complexity makes it difficult for existing methods to identify the formula with correct mathematical forms.

To solve this problem, in this work we proposed a new search objective inspired by the minimum description length (MDL) (Kolmogorov, 1963), which represents the size of the simplest model used to describe the data, or, in SR, the minimum number of symbols required for the target formula $y = f(x)$. If each mathematical symbol is regarded as a transformation step, then MDL describes the number of transformations needed to go from the independent variable, x , to the dependent variable, y . Therefore, the search with minimal MDL as the optimization objective has an optimal substructure (Cormen et al., 2022): only when the correct transformation is executed can the MDL reduce, thus the search direction of MDL reduction is always consistent with the direction leading to the target formula (see Figure 1). However, MDL has been shown to be incomputable (Vitányi, 2020), indicating that no algorithm can provide an accurate MDL for arbitrary input. Nevertheless, the capacity of neural networks as universal approximators (Nielsen, 2015) indicates that, with sufficient data, a suitably designed neural network can effectively learn the complex mapping from the data to its MDL. To this end, we developed a Transformer-based neural network, MDLformer. Through large-scale training on over 130 million symbolic-numeric pairs using a carefully designed training strategy that aligns the numerical space with the symbolic space, MDLformer has gained the ability to estimate the MDL of any given data. With the search objective provided by the large-scale trained MDLformer, we implement a new SR method based on the Monte Carlo tree search algorithm (Browne et al., 2012), a heuristic search algorithm that has been proven to be suitable for use in conjunction with neural networks successfully by many works (Silver et al., 2016, 2017; Kamienny et al., 2023).

We conduct extensive experiments to illustrate the excellent performance of our approach in recovering formulas from data. Across two problem sets with 133 formulas, our method successfully recovers around 50 of them, outperforming state-of-the-art methods by 43.92%. We also find this result robust to noise: even if we add noise with an intensity of 10% to the data, the recovery rate of our method is still higher than the recovery of other methods in the absence of noise. We also test our method on the black-box problem sets, finding it can discover formulas that describe the data with lower description length and higher accuracy than other methods. Further analysis of the MDLformer demonstrates its scalable and robust capability for accurate predictions of the MDL, which explains the outstanding performance of our SR method.

2 Related Work

Heuristic search methods. Traditionally, symbolic regression approaches are mainly based on the genetic programming (GP) algorithms (Langdon & Poli, 2013), which maintains a set of symbolic formulas and iteratively updates these candidate formulas via mutation and crossover operations. To this day, there have been plenty of GP-based symbolic regression toolkits developed, such as Eureqa (Dubčáková, 2011), GPLEarn (Stephens, 2016), PySR (Cranmer, 2023), and so on (Schmidt & Lipson, 2010; de Franca & Aldeia, 2021; La Cava et al., 2016; Arnaldo et al., 2014; Virgolin et al., 2019, 2021; Burlacu et al., 2020; Zhong et al., 2018; Zhang et al., 2022; Augusto & Barbosa, 2000; Kartelj & Djukanović, 2023; Smits & Kotanchek, 2005; Searson et al., 2010). In these years, people have begun to use reinforcement learning algorithms for symbolic regression, including Monte-Carlo tree search (MCTS) (Sun et al., 2022), double Q-learning (Xu et al., 2024), and deep reinforcement learning (DRL) (Petersen et al., 2021; Tenachi et al., 2023). These methods start from the empty formula and iteratively select appropriate mathematical symbols to fill in until a complete formula is obtained. Some works combine multiple methods to achieve better symbol regression (Mundhenk et al., 2021; Jin et al., 2020; McConaghy, 2011; Landajuela et al., 2022). These search algorithms, however, all face the problem that the prediction errors usually do not decrease monotonically from the initial state to the ground-truth formula. Although recent methods introduced formula complexity as a regularization term alongside the prediction error (Sun et al., 2022; Cranmer, 2023), this problem persists and their recovery rates remain low. In contrast, our approach addresses this problem by optimizing the minimum description length (MDL), which decreases monotonically along the path to the target formula.

Neural network-assisted search methods. Recently, some works have attempted to enhance the search methods by utilizing the powerful fitting capabilities of neural networks. For example, Mundhenk et al. (2021) proposes to train an RNN by deep reinforcement learning to generate the initial candidate formulas in genetic algorithms for speeding up evolution. While Kamienny et al. (2023) utilizes a Transformer pre-trained as a next-symbol predictor to provide promising search directions for the Monte Carlo tree search algorithm. Although these works still take prediction error as the search goal and thus do not have optimal substructure, they inspire us to combine pre-trained neural networks with search algorithms. AIFeynman shows another way to combine neural networks and search algorithms (Udrescu & Tegmark, 2020; Udrescu et al., 2020): it discovers symmetry properties in data by fitting it with neural networks and, based on this, converts the search for the target formula into searches for several smaller subformulas. However, leveraging hand-designed symmetry properties summarized on the Feynman dataset, AIFeynman cannot be adapted to other datasets without these properties, and these rules are sensitive to noise, making AIFeynman’s recovery rate decrease significantly on noisy data (Cavalab, 2022). As a comparison, our method can also be regarded as a method of recursively simplifying the target function, since the decrease of MDL indicates a candidate formula f as a subformula of the target one. Identifying subformulas based on MDLformer’s output rather than hand-designed rules, our method does not rely on specific prior knowledge and is more robust to noise.

Regression and generative methods using neural networks. In addition to using neural networks to assist search, some works proposed neural network-based regression methods. They design fully connected neural networks with mathematical functions, such as \sin , \exp , \times , as activation layers. After fitting weight parameters to the input data, they can extract mathematical formulas from the networks Kim et al. (2020); La Cava et al. (2019); Kubalík et al. (2023). However, due to using mathematical functions like exponential and logarithmic functions as activation layers, these methods usually face numerical instability problems such as gradient explosion. Other works are based on generative methods. They use large-scale pre-trained Transformers to generate symbolic sequences as target formulas from the data directly (Biggio et al., 2021; Kamienny et al., 2022; Meidani et al., 2023; Bendinelli et al., 2023; d’Ascoli et al., 2022). Once pre-trained, these methods can directly generate target formulas without searching or extra training. Therefore, they are usually faster than other methods. However, it is still difficult for them to obtain the target formula with the correct form, since small changes in the input data can lead to completely different objective functions (Kamienny et al., 2023). As a comparison, based on the search method, our approach can improve the results through extended running durations, and the utilization of the MDL search objective enhances its efficiency, allowing it to achieve a high recovery rate for the target formula within a reasonable timeframe.

3 Learning to Estimate Formula Complexity with MDLformer

3.1 MDLformer

The design of MDLformer is rooted in the recent development of Transformer models, which have been proven to be able to encode numeric observation data into latent space, which can be further used for inferring corresponding symbolic formulas (Biggio et al., 2021; Kamienny et al., 2022). Meidani et al. (2023) further find that, by aligning the latent spaces of two Transformer models that encode numeric data and symbolic formulas, respectively, it’s possible to

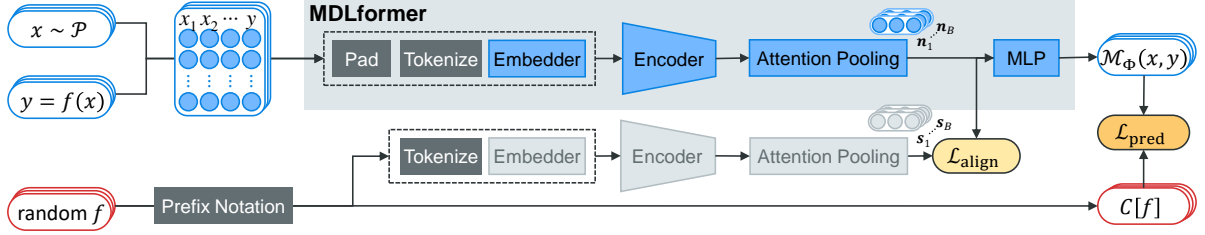


Figure 2: Schematic diagram of the architecture and learning process of MDLformer.

predict cross-model properties. Here we exploit this approach to cross-modally predict the length of the corresponding symbolic formula, i.e., the minimum description length (MDL), based on numeric observational data,

As depicted in Figure 2, the MDLformer, \mathcal{M}_Φ , integrates an embedder, a Transformer encoder, an attention-based pooling, and a multilayer perceptron (MLP) as readout head, to map the input data $x \in \mathbb{R}^{N \times D}$ and $y \in \mathbb{R}^{N \times 1}$ into its MDL, $C[f]$, where f denotes the simplest symbolic function that describes $y = f(x)$ and $C[f]$ is its complexity, i.e., the number of symbols required to express f .

Embedding. We first pad x into $\mathbb{R}^{N \times D_{\max}}$ with zeros since the number of features D can vary. We then tokenize the input data using base-10 floating-point notation. Specifically, we round each value to 4 significant digits and then split it into three parts: sign (+, -), mantissa (0.000 ~ 9.999), and exponent ($E-100 \sim E+100$). For example, a value 54.321 is represented as a sequence $[+, 5.432, E+1]$. The input data is tokenized into $N \times (D_{\max} + 1) \times 3$ tokens, which, increases with N and D_{\max} , challenges the quadratic complexity of Transformers. Therefore, we sample no more than N_{\max} pairs from each row of x and y and then embed each x-y pair into the latent space with a fixed dimensionality d_f to feed into the Transformer encoder.

Encoding. We leverage a Transformer encoder (Vaswani et al., 2017) to process the embedded numeric input. Notably, we remove the positional encoding in the numeric encoder since each item in the input sequence represents a pair of x-y data and their order is thus not important, which aligns with the previous practices (Biggio et al., 2021; Kamienny et al., 2022; Meidani et al., 2023).

Pooling. To map the Transformer encoder’s outputs, $V \in \mathbb{R}^{N \times d_f}$, into a fixed-size representation, we adopt an attention-based pooling mechanism (Santos et al., 2016). Specifically, we use a learnable weight, $w \in \mathbb{R}^{d_f}$, to calculate an attention weight for each row $v_i \in V$ by $a_i = \text{softmax}(w \cdot v_i)$, where the softmax is conducted along the sequence dimension N . Then, we add them up with a_i as weights to get the final representation: $n = \sum_i a_i v_i$.

Reading out. After pooling we obtain a compact representation for the whole numeric input, which can be used to predict cross-model properties (Meidani et al., 2023). Here we predict the MDL with a multilayer perceptron that uses ReLU as the activation layer.

3.2 Training Data Generation

The training of the MDLformer relies on plenty of paired numeric and symbolic data, which is generated during the learning process on the fly. During the whole process, we generate a total of about 131 million pairs of input data.

Generate symbolic formulas. We generate symbolic formulas with the algorithm proposed by Kamienny et al. (2022) to ensure diversity: First, we sample the number of features, $D \sim \mathcal{U}\{0, \dots, D_{\max}\}$. Then, we randomly combine them with b binary operators and further sample u unary operators to insert into the random position of the resulting formula. Finally, we add non-similar transformations to each position of the formula: $f_i \mapsto a_i f_i + b_i$, where f_i are subformulas of f , a_i and b_i are sampled from $\mathcal{U}[-100, 100]$. To ensure that f is in its simplest form, we simplify it with sympy, an open-source Python package for algebra processing.

Generate numeric data. After generating the formula, we sample the number of features, D , from $\mathcal{U}\{1 \dots D_{\max}\}$ and generate numeric data for D independent variables: $x \in \mathbb{R}^{N \times D} \sim \mathcal{P}$. Then, we calculate corresponding numeric data for the dependent variable: $y = f(x) \in \mathbb{R}^{N \times 1}$. Considering that f ’s domain cannot be the whole \mathbb{R}^D when it contains specific operators, such as logarithm or square root, some of the sample points in x may not be in its domain and lead to invalid dependent variable values. Therefore, we discard invalid values in y and the corresponding rows in x , ensuring each sample point of x lies in the domain of f . We also find that the choice of \mathcal{P} can significantly influence the performance of MDLformer when using it for symbolic regression. We use the Gaussian mixture model (GMM) as suggested by Kamienny et al. (2022), which takes the sum of C Gaussian distributions with random mean and variance

and normalizes them as the distribution \mathcal{P} . To further improve the diversity of numerical data and enhance its prediction performance in actual symbolic regression, we also considered another sampling method, that is, generating it by a function transformation on hidden variables z . Specifically, we first sample $z \in \mathbb{R}^{N \times K}$ from a GMM distribution, and then generate a random symbolic function $g \sim \mathcal{F}_{\mathcal{K} \times \mathcal{D}}$ following the methods introduced above, and finally operate the hidden variable with the function to obtain $x = g(z) \in \mathbb{R}^{N \times D}$. This design comes from the fact that, when using MDLformer for symbolic regression, we need to estimate the minimal description length of the transformation results obtained by operating symbolic functions on the input data x .

3.3 Cross-Modal Learning for Formula Complexity

With the generated formulas f_i and data (x_i, y_i) , we train the MDLformer using two learning objectives, including a primary objective that predicts the accurate MDL and an auxiliary objective that aligns the numeric latent space and the symbolic latent space, as depicted in Figure 2.

Primary learning objective for prediction. To train the MDLformer for predicting the corresponding minimum description length (MDL) based on numerical input, we optimize the mean square error, $\mathcal{L}_{\text{pred}}$, between MDLs estimated by the MDLformer and ground-truths:

$$\mathcal{L}_{\text{pred}} = \frac{1}{B} \sum_{i=1}^B (C[f_i] - \mathcal{M}_{\Phi}(x_i, y_i))^2, \quad (1)$$

where B denotes the batch size, $C[f_i]$ is the complexity of the symbolic function f_i .

Alignment as an auxiliary learning objective. The auxiliary objective, proposed by Meidani et al. (2023), aims to facilitate a mutual understanding of both numeric and symbolic domains and thus empower better cross-modal prediction. Specifically, as suggested by Meidani et al. (2023), we introduce a symbolic encoder to map the prefix notation of f into a compact representation s , which has a structure similar to the numeric encoder, as depicted in Figure 2. The latent spaces of these two encoders are aligned by optimizing a symmetric cross-entropy loss over similarity scores:

$$\mathcal{L}_{\text{align}} = - \left(\sum_{i=1}^B \log \frac{\exp(\mathbf{n}_i \cdot \mathbf{s}_i / \tau)}{\sum_{j=1}^B \exp(\mathbf{n}_i \cdot \mathbf{s}_j / \tau)} + \sum_{i=1}^B \log \frac{\exp(\mathbf{s}_i \cdot \mathbf{n}_i / \tau)}{\sum_{j=1}^B \exp(\mathbf{s}_i \cdot \mathbf{n}_j / \tau)} \right), \quad (2)$$

where τ is the temperature parameter, \mathbf{s}_i and \mathbf{n}_i are encoded representations of i -th numeric data and symbolic function, respectively.

Training Strategy We adopt a two-step training strategy: First, we train the MDLformer with the auxiliary objective and the generated formula-data pairs, where the numeric data is sampled from the GMM. ii) Then, we use the primary objective to train the MDLformer on the numeric data generated by operating symbolic functions on latent variables. The first step aligns the latent space of the numerical encoder and the symbolic encoder and thus provides a good start for the numerical encoder to predict the formula length in the symbolic space cross-modally. Based on this, the second step uses a data distribution that is closer to the actual symbolic regression used, allowing the data encoder to estimate the description complexity of the input data accurately.

4 MDL-guided Symbolic Regression with MDLformer

In this section, we explain how the trained MDLformer can help symbolic regression discover target formulas with correct mathematical forms more easily. The main idea is to change the search direction from the direction of prediction error reduction to the direction of minimum description length (MDL) reduction. This leads to the property of optimal substructure and makes it easier for the existing search algorithms to search for the target formula with the correct form.

4.1 Searching for Minimum Description Length

As depicted in Figure 3, existing search-based methods focus on the update-and-select loops over a set of candidate formulas: after generating an initial formula set, $\{f_{0,i} \in \mathcal{F}_{D \times 1}\}$, these methods generate algorithm-specific symbolic functionals $F_{k,i} : \mathcal{F}_{D \times 1} \rightarrow \mathcal{F}_{D \times 1}$ (such as the crossover and mutation in genetic programming, see B for details.) to creating new candidate formulas: $f'_{k+1,i} = F_{k,i}(f_{k,i})$, and select resulting functions with low prediction errors for the next round of iteration. This update-and-select loop is repeated iteratively until a formula with a low enough prediction error is encountered, at that point the loop will terminate and this formula will be read out as a result: $f^* = \arg \min_f \|y - f(x)\|^2$.

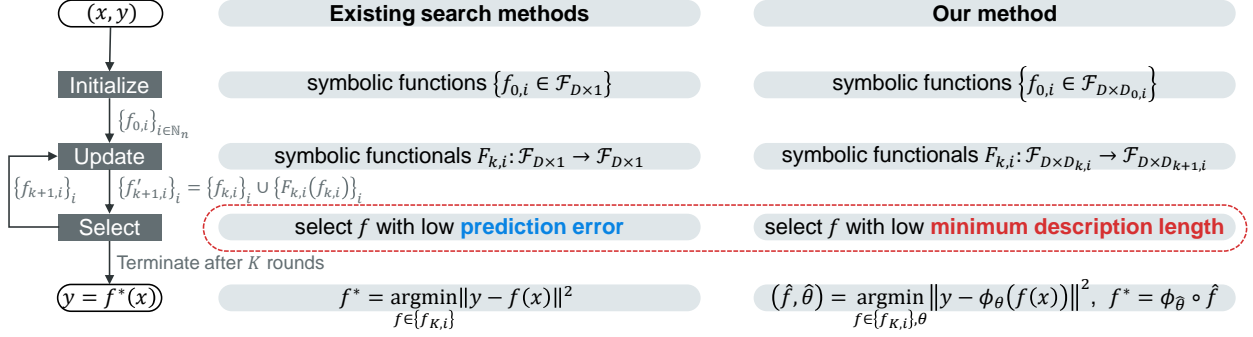


Figure 3: **Comparison of existing search methods and our method.** $x \in \mathbb{R}^{N \times D}$ and $y \in \mathbb{R}^{N \times 1}$ are observational data, $\mathcal{F}_{p \times q}$ denotes all possible symbolic functions mapping from $\mathbb{R}^{N \times p}$ to $\mathbb{R}^{N \times q}$. $i \in \mathbb{N}_n$ denotes the indexes of candidate formulas (in a total of n), while k denotes the number of loops (terminated at round K). $T_{k,i}$ are algorithm-specific symbolic functionals, like crossover and mutation operations in GP, whose concrete operations in different search algorithms are summarized in Table 3. ϕ_θ are simple functions (like linear functions) with parameters θ that map f into $\mathcal{F}_{D \times 1}$.

In contrast, instead of maintaining a candidate set of target formulas, we maintain a candidate set of *subformulas* of the target formula, $\{f_{k,i} \in \mathcal{F}_{D \times D_{k,i}}\}$. For a candidate $f \in \{f_{k,i}\}$, each of its item $f^{(d)}$ denotes a part of the target, i.e., $f^* = \phi(f_{k,i}) = \phi(f^{(1)}, f^{(2)}, \dots, f^{(D_{k,i})})$. ϕ reflects the transformation required from f to the target formula f^* , while its complexity, $C[\phi]$, evaluates the “distance” between $f_{k,i}$ and f^* . Therefore, by selecting $f_{k,i}$ with low MDL estimated by the MDLformer, $\mathcal{M}_\Phi(f_{k,i}(x), y) \approx C[\phi]$, during the update-and-select loops, the remaining transformation ϕ can be simplified iteratively, and thus the candidates f will get “closer” to the target one. For an $f_{K,i}$ that is sufficiently close to f^* after K iterations, the remaining transformation from $f_{K,i}$ to f^* can be described by a simple parameterized function ϕ_θ accurately (θ are parameters). Formally speaking, we find

$$(\hat{f}, \hat{\theta}) = \arg \min_{f \in \{f_{K,i}\}, \theta} \|y - \phi_\theta(f(x))\|^2 \quad (3)$$

from the candidate set to determine the target formula: $f^* = \phi_{\hat{\theta}}(\hat{f})$.

4.2 Implementation

In this work, we implement our method based on the Monte Carlo tree search (MCTS) (Browne et al., 2012) because of its application in symbolic regression task (Sun et al., 2022) as well as its successful combination with neural networks in numerous studies (Kamienny et al., 2023; Silver et al., 2016, 2017). MCTS is a classical heuristic search algorithm that maintains a search tree with each node representing a candidate formula and updates the tree through four steps: selection, expansion, simulation, and backpropagation. The vast majority of our implementations are consistent with the existing practice of using MCTS for symbolic regression (Sun et al., 2022), except that the upper confidence bound (UCB) to guide the search is based on MDLformer’s output (see Appendix B for details). For the remaining transformation ϕ_θ , we use the simplest linear function:

$$\phi_\theta(f_{k,i}) = \sum_{d=1}^{D_{k,i}} \theta_d f^{(d)}, \quad (4)$$

where $f^{(d)} \in \mathcal{F}_{D \times 1}$ is the d -th item of $f_{k,i}$. Though it is possible to use functions in other forms, such as multiplications or polynomials, or even brute force searches used by AIFeynman (Udrescu & Tegmark, 2020), we find that even the simplest linear functions work well enough as long as MDLformer’s estimation is accurate enough.

5 Experiments

5.1 Symbolic Regression on Ground-Truth Problems

We evaluate our method on the SRbench (La Cava et al., 2021) as most of the previous work does, which contains 252 regression datasets from Penn Machine Learning Benchmark (PMLB) (Olson et al., 2017) in three types: 122 black-box problems without known underlying formulas, and both 14 Strogatz problems (Strogatz, 2018) and 119

Table 1: **Recovery rate and search time of different methods in both Strogatz and Feynman datasets.** Each experiment is conducted at ten random seeds and four noise levels.

Type	Method	Strogatz (14 problems)		Feynman (119 problems)	
		R. Rate \uparrow	Time (s)	R. Rate \uparrow	Time (s)
Regression	FEAT (La Cava et al., 2019)	0.19%	636.6	0.00%	1532
Generative	NeurSR (Biggio et al., 2021)	1.79%	15.71	2.44%	24.78
	E2ESR (Kamienny et al., 2022)	3.78%	4.044	10.40%	4.576
	SNIP (Meidani et al., 2023)	6.79%	1.457	1.60%	2.196
Search-based	GPlearn (Stephens, 2016)	9.21%	966.2	16.89%	3349
	AFP (Schmidt & Lipson, 2010)	10.90%	160.7	17.51%	3845
	AFP-FE (Schmidt & Lipson, 2010)	12.86%	9532	20.80%	25138
	EPLEX (La Cava et al., 2016)	6.02%	446.8	10.10%	11548
	SBP-GP (Virgolin et al., 2019)	2.44%	20089	2.88%	28933
	GP-GOMEA (Virgolin et al., 2021)	8.46%	1100	10.32%	3456
	Operon (Burlacu et al., 2020)	4.29%	83.58	7.97%	2656
	SPL (Sun et al., 2022)	8.12%	363.7	10.48%	263.3
	DSR (Petersen et al., 2021)	18.05%	784.3	18.60%	1042
	RSRM (Xu et al., 2024)	4.43%	133.2	15.40%	127.1
	AlFeynman2 (Udrescu et al., 2020)	15.27%	241.3	27.24%	708.6
	BSR (Jin et al., 2020)	0.38%	25346	0.70%	30635
	Ours	66.78%	338.3	33.93%	660.5
		(+6.82 formulas)		(+7.96 formulas)	

Feynman problems (Udrescu & Tegmark, 2020) with known ground-truth underlying formulas. Since we mainly focus on the recovery rate, that is, how often an algorithm can find the correct formula with a mathematically equivalent form to the target formula, we consider the last two ground-truth problems. We compare 16 baseline algorithms split into three types: the generative methods and the regression methods, both of which are based on neural networks, as well as the search methods using genetic programming or reinforcement learning. (see Appendix C.1.1 for details). For each algorithm on each problem, we test its performance from 10 fixed random seeds at 4 different noise levels: $\epsilon = 0.0, 0.001, 0.01, 0.1$.

The experiment results are provided in Table 1, where our method reaches the top recovery rate in both problem sets with reasonable search time. In the Strogatz problem set, our method improves the Recovery Rate from 15.27% to 66.17%, increasing nearly three times. In the Feynman problem set, our method also improves the Recovery Rate by 11.94%. Overall, our method recovers around 50 formulas out of 133, outperforming the best baseline (35 formulas by AlFeynman2) by 43.92%.

In Figure 4 we also plot the recovery rate of all methods at different noise levels (see Appendix C.1.2 for details). On the Strogatz problem set, our method has the highest recovery rate that significantly surpasses other methods. On the Feynman problem set, however, AlFeynman2 shows a higher recovery rate than our methods when the noise level is 0.0. This is because AlFeynman2 designs a series of rules based on the characteristics of formulas in the Feynman problem set to help search for formulas. In contrast, as a general method with no reliance on any prior knowledge, our method can be directly applied to different problem sets. Furthermore, unlike AlFeynman, which experiences a sharp decline in performance due to the failure of hand-designed rules in the presence of noise, our method is robust to noise: Even at the maximum noise level ($\epsilon = 0.1$), our method still outperforms other methods without noise, including the AlFeynman2 on the Strogatz dataset.

5.2 Symbolic Regression on Black-Box Problems

We also test our method on 122 black-box problems from SRbench. Unlike ground-truth problems, in these problems, there are no underlying formulas describing the patterns in data. Therefore, we split the data of each problem into 75% training set and 25% test set, and, instead of recovery rate, we evaluate the results using the Pareto front that balances the test set accuracy and the formula complexity, which is a common practice in SR tasks Cavalab (2022). For the baseline methods, in addition to the three types of methods considered in the ground-truth problem set, we also consider decision tree-based methods (see Appendix C.1.1 for details), where the constructed decision trees are treated as a generalized formula tree that uses conditional selection as operators and the number of nodes in the trees are used as the formula complexity.

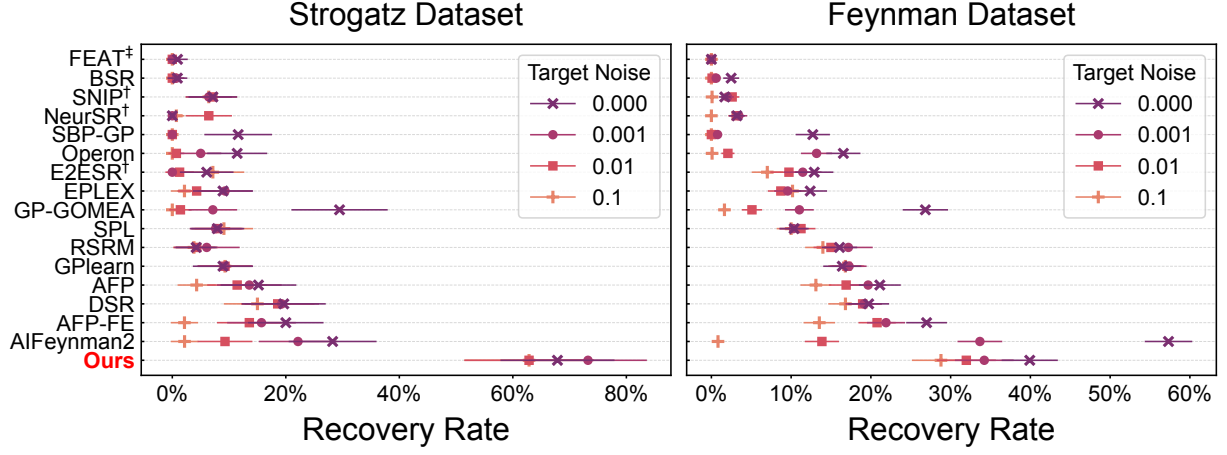


Figure 4: **Recovery rate at different noise levels.** [†] and [‡] denote generative and regression methods, the others are search methods. The error bars depict the 95% confidence interval.

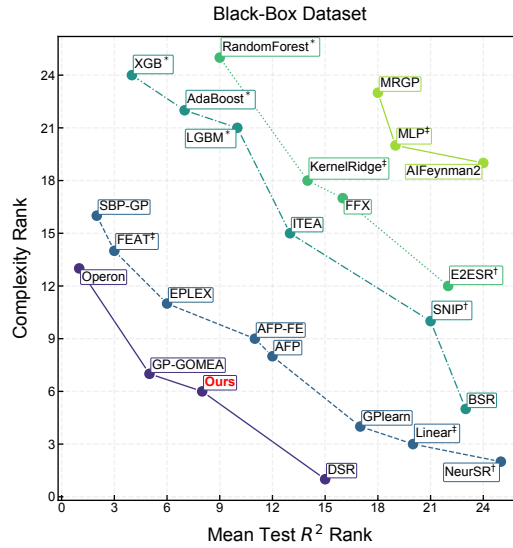


Figure 5: **Pareto fronts on black-box dataset.** [†], [‡], and * denote generative, regression, and decision-tree methods, respectively, the others are search methods. The colored lines mark the Pareto front in different ranks, from bottom left (best) to upper right (worst).

The overall performance of our method and other baselines is shown in Figure 5, where we can see that, our method achieves a higher test set R^2 with lower model complexity than other methods and is thus sharing the first rank of the Pareto front with three other search algorithms, that is, Operon (Burlacu et al., 2020), GP-GPMEA (Virgolin et al., 2021), and DSR (Petersen et al., 2021). In contrast, decision tree methods or regression methods usually construct formulas that are too complex and lack interpretability to describe the given data; while generative methods are unable to iteratively optimize the results and thus have low test set accuracy.

5.3 MDLformer Performance

We report the prediction performance of MDLformer by evaluating it on $K = 1024$ pairs of symbolic formulas and numeric data generated as described in Section 3.2, where the independent variables x are sampled from GMM. Given that the relative relationship of predicted values is more important than their absolute magnitudes when using MDLformer to guide symbolic regression, we consider ranking metrics in addition to the commonly used root mean squared error (RMSE) and coefficient of determination (R^2). Particularly, we consider the area under the ROC curve (AUC) (Fawcett, 2006), which assesses the likelihood that the predicted values and true values maintain consistent ordering when randomly selecting pairs (formalized in Appendix C.2.1). where \mathbb{I} is the indicator function. As shown in Table 2, the RMSE metric indicates an average error of 3.9, which is only 15% of the average formula length of 25. The R^2 and AUC are also close to 1.0, demonstrating the excellent performance of MDLformer in predicting the complexity of formulas corresponding to the data. We also provide the results of the other three metrics in Appendix C.2.1.

MDLformer indicates correct search directions. Here we use a case study to illustrate that the minimum description length (MDL) estimated by MDLformer has the optimal substructure, that is: 1) the subformula of the target formula has a lower MDL than other formulas and 2) the MDL monotonically decreases along the construction route of the target formula f . As shown in Figure 6, we consider the Feynman I.18.4 equation, where the target formula can be obtained from five steps of transformations $T_{0:4}^*$. Specifically, starting from $d_0 \equiv x$, we iteratively operate the transformation T_i^* that eventually maps d_0 to $d_5 \equiv y$. For each d_i , we estimate its MDL concerning y with the MDLformer and plot the result in the red line, finding the estimated MDL does monotonically decrease as the formula form gets closer to the target formula. For each d_i , we also draw the estimated MDL of $d' = T'(d_i)$ for all possible symbolic functions T' as the blue sectors, finding that nearly few of d' has a lower MDL than the correct transformation result of $d_{i+1}^* = T_i^*(d_i)$, indicating the correct search direction is consistent with the direction in which MDL decreases the fastest.

Ablation study on training strategy. Figure 7a shows the ablation experiment on the training strategy. We considered three strategies to train the MDLformer with the alignment objective $\mathcal{L}_{\text{align}}$ and the prediction objective $\mathcal{L}_{\text{pred}}$: 1) sequentially training for alignment and then prediction (i.e., the training scheme described in Sec 3.3), 2) training for alignment and prediction concurrently, and 3) direct training for prediction without alignment. A total of 1000 rounds of training were performed for each of the three wheres, where for the first method, the first 500 rounds are for alignment and the last 500 rounds are for prediction. Among them, the first two strategies have lower RMSE than the last one, demonstrating that aligning numerical and symbolic spaces improves cross-model prediction, which is consistent with the observation of previous work (Meidani et al., 2023). The Sequential strategy has a lower RMSE than the Concurrent strategy, which may be because it is more difficult to use both objectives at the same time. Figure 7b shows the relationship between the prediction error and the number of input points N , demonstrating that more data can help MDLformer predict the minimum description length more accurately. However, a larger N can lead to an increase in inference time, thus we choose $N = 200$ to balance the accuracy and efficiency.

Table 2: **Prediction performance of MDLformer.**

RMSE	R^2	AUC
3.9105	0.9035	0.8859

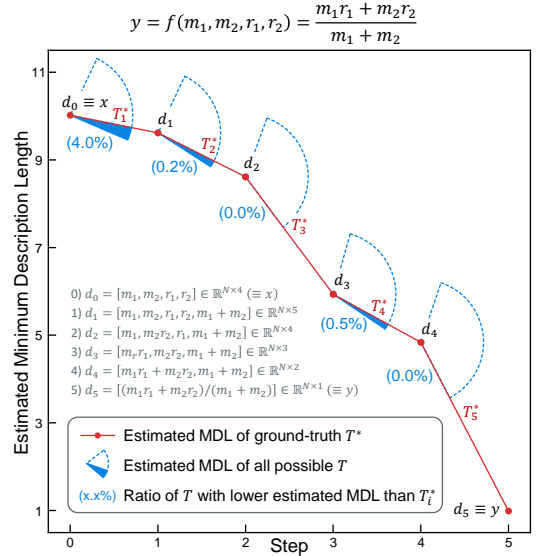


Figure 6: **A case study of Feynman I.18.4 equation.** A series of symbolic functions T_i^* map $d_0 \equiv x$ to $d_5 \equiv y$ iteratively. The red line shows, $\mathcal{M}_\Phi(d_i, y)$, the estimated MDL of each d_i . The blue sectors show the estimated MDL of all possible symbolic functions $d' = T'(d_i)$, among which only a few have lower MDL than T_i^* as annotated by the percentage value.

Consistent predictive capability across task difficulty. In Figure 7d,e,f we measure the predictive performance of MDLformer on formulas of different difficulty, indicated by 1) the number of variables, 2) the number of unary operators, and 3) the number of binary operators. Although RMSE, consistent with intuition, increases with the formula difficulty. But considering that more difficult formulas can have longer lengths, we additionally plot the ratio of $RMSE$ to the average formula length, \bar{L} , in the graph. It can be seen that as the formula difficulty increases, the normalized RMSE remains basically unchanged, indicating that our MDLformer scales well with the formula difficulty.

Robustness against noise. In Figure 7c we add feature noise to the data of independent variables: $x \leftarrow x + n$, where $n \sim \mathcal{N}(0, \eta\sigma_x)$ is additive noise with intensity proportional to the standard deviation of x , σ_x . We find that although the RMSE increases with the noise intensity, the ranking metric, AUC, basically remains unchanged as noise increases, suggesting that our method can identify the relative magnitude of MDL even under noisy conditions. Considering that the search process relies solely on the relative magnitude of estimated MDL, this explains the reason for the robustness of our method to noise in Section 5.1.

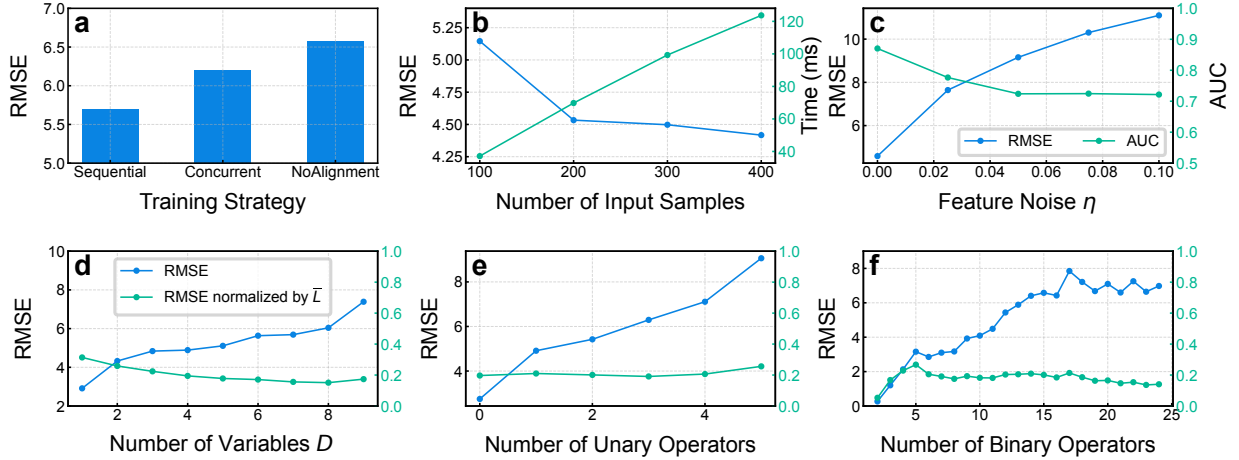


Figure 7: **Ablation Study.** The prediction performance of MDLformer with respect to **a**: trained with three alignment strategies, **b**: number of input pairs N , **c**: feature noise η , **d**: number of variables D , **e**: number of unary operators, and **f**: number of binary operators. In **d,e,f** we also plot the RMSE normalized by the average formula length \bar{L} .

6 Discussion and Conclusion

In this work, we introduce SR4MDL, a symbolic regression approach that optimizes for minimum description length (MDL) rather than prediction error. Leveraging the impressive prediction capabilities of MDLformer, it successfully recovers around 50 formulas across two benchmark datasets comprising 133 problems, outperforming state-of-the-art methods by 43.92%. Additionally, it ranks in the top tier for finding formulas that balance accuracy and complexity on a black-box problem set with 122 problems. While SR4MDL showcases robustness and versatility in searching for correct formulas in a near-optimal direction, it has notable limitations. First, the performance of MDLformer on data with complex relationships needs to be improved. Second, although the increased efficiency caused by the MDLformer makes our method faster than the regression methods, it is still lower than generative methods. Despite these limitations, SR4MDL offers a wide range of capabilities, making it a powerful tool for uncovering symbolic laws that underlie diverse complex systems.

References

- Dimitrios Angelis, Filippas Sofos, and Theodoros E Karakasidis. Artificial intelligence in physical sciences: Symbolic regression trends and perspectives. *Archives of Computational Methods in Engineering*, 30(6):3845–3865, 2023.
- Ignacio Arnaldo, Krzysztof Krawiec, and Una-May O’Reilly. Multiple regression genetic programming. In *Proceedings of the 2014 Annual Conference on Genetic and Evolutionary Computation*, pp. 879–886, 2014.
- Douglas Adriano Augusto and Helio JC Barbosa. Symbolic regression via genetic programming. In *Proceedings. Vol. 1. Sixth Brazilian symposium on neural networks*, pp. 173–178. IEEE, 2000.

- Tommaso Bendinelli, Luca Biggio, and Pierre-Alexandre Kamienny. Controllable neural symbolic regression. In *ICML*, pp. 2063–2077. PMLR, 2023.
- Luca Biggio, Tommaso Bendinelli, Alexander Neitz, Aurelien Lucchi, and Giambattista Parascandolo. Neural symbolic regression that scales. In *ICML*, pp. 936–945. PMLR, 2021.
- Cameron B Browne, Edward Powley, Daniel Whitehouse, Simon M Lucas, Peter I Cowling, Philipp Rohlfshagen, Stephen Tavener, Diego Perez, Spyridon Samothrakis, and Simon Colton. A survey of monte carlo tree search methods. *IEEE Transactions on Computational Intelligence and AI in games*, 4(1):1–43, 2012.
- Bogdan Burlacu, Gabriel Kronberger, and Michael Kommenda. Operon c++ an efficient genetic programming framework for symbolic regression. In *Proceedings of the 2020 Genetic and Evolutionary Computation Conference Companion*, pp. 1562–1570, 2020.
- Cavalab. Srbench: A living benchmark framework for symbolic regression, 2022. URL <https://cavalab.org/srbench/results/#symbolically-verified-solutions>. Accessed: 2024-09-26.
- Tianqi Chen and Carlos Guestrin. Xgboost: A scalable tree boosting system. In *Proceedings of the 22nd acm sigkdd international conference on knowledge discovery and data mining*, pp. 785–794, 2016.
- Yize Chen, Marco Tulio Angulo, and Yang-Yu Liu. Revealing complex ecological dynamics via symbolic regression. *BioEssays*, 41(12):1900069, 2019.
- Thomas H Cormen, Charles E Leiserson, Ronald L Rivest, and Clifford Stein. *Introduction to algorithms*. MIT press, 2022.
- Cristina Cornelio, Sanjeeb Dash, Vernon Austel, Tyler R Josephson, Joao Goncalves, Kenneth L Clarkson, Nimrod Megiddo, Bachir El Khadir, and Lior Horesh. Combining data and theory for derivable scientific discovery with ai-descartes. *Nature Communications*, 14(1):1777, 2023.
- Miles Cranmer. Interpretable machine learning for science with pysr and symbolicregression.jl. *arXiv preprint arXiv:2305.01582*, 2023.
- Stéphane d’Ascoli, Pierre-Alexandre Kamienny, Guillaume Lample, and François Charton. Deep symbolic regression for recurrent sequences. *ICML*, 2022.
- Fabricio Olivetti de Franca and Guilherme Seidyo Imai Aldeia. Interaction–transformation evolutionary algorithm for symbolic regression. *Evolutionary computation*, 29(3):367–390, 2021.
- Renáta Dubčáková. Eureqa: software review, 2011.
- Tom Fawcett. An introduction to roc analysis. *Pattern recognition letters*, 27(8):861–874, 2006.
- Yoav Freund and Robert E Schapire. A decision-theoretic generalization of on-line learning and an application to boosting. *Journal of computer and system sciences*, 55(1):119–139, 1997.
- Ying Jin, Weilin Fu, Jian Kang, Jiadong Guo, and Jian Guo. Bayesian symbolic regression. *AAAI*, 2020.
- Pierre-Alexandre Kamienny, Stéphane d’Ascoli, Guillaume Lample, and François Charton. End-to-end symbolic regression with transformers. *NeurIPS*, 35:10269–10281, 2022.
- Pierre-Alexandre Kamienny, Guillaume Lample, Sylvain Lamprier, and Marco Virgolin. Deep generative symbolic regression with monte-carlo-tree-search. In *ICML*, pp. 15655–15668. PMLR, 2023.
- Aleksandar Kartelj and Marko Djukanović. Rils-rols: Robust symbolic regression via iterated local search and ordinary least squares. *Journal of Big Data*, 10(71), 2023. doi: 10.1186/s40537-023-00743-2.
- Guolin Ke, Qi Meng, Thomas Finley, Taifeng Wang, Wei Chen, Weidong Ma, Qiwei Ye, and Tie-Yan Liu. Lightgbm: A highly efficient gradient boosting decision tree. *Advances in neural information processing systems*, 30, 2017.
- Samuel Kim, Peter Y Lu, Srijon Mukherjee, Michael Gilbert, Li Jing, Vladimir Čeperić, and Marin Soljačić. Integration of neural network-based symbolic regression in deep learning for scientific discovery. *IEEE transactions on neural networks and learning systems*, 32(9):4166–4177, 2020.
- Andrei N Kolmogorov. On tables of random numbers. *Sankhyā: The Indian Journal of Statistics, Series A*, pp. 369–376, 1963.
- Jiří Kubalík, Erik Derner, and Robert Babuška. Toward physically plausible data-driven models: a novel neural network approach to symbolic regression. *IEEE Access*, 11:61481–61501, 2023.
- William La Cava, Lee Spector, and Kourosh Danai. Epsilon-lexicase selection for regression. In *Proceedings of the Genetic and Evolutionary Computation Conference 2016*, pp. 741–748, 2016.
- William La Cava, Tilak Raj Singh, James Taggart, Srinivas Suri, and Jason H Moore. Learning concise representations for regression by evolving networks of trees. *ICLR*, 2019.

- William La Cava, Bogdan Burlacu, Marco Virgolin, Michael Kommenda, Patryk Orzechowski, Fabrício Olivetti de França, Ying Jin, and Jason H Moore. Contemporary symbolic regression methods and their relative performance. *Advances in neural information processing systems*, 2021(DB1):1, 2021.
- Mikel Landajuela, Chak Shing Lee, Jiachen Yang, Ruben Glatt, Claudio P Santiago, Ignacio Aravena, Terrell Mundhenk, Garrett Mulcahy, and Brenden K Petersen. A unified framework for deep symbolic regression. *Advances in Neural Information Processing Systems*, 35:33985–33998, 2022.
- William B Langdon and Riccardo Poli. *Foundations of genetic programming*. Springer Science & Business Media, 2013.
- Sannyuya Liu, Qing Li, Xiaoxuan Shen, Jianwen Sun, and Zongkai Yang. Automated discovery of symbolic laws governing skill acquisition from naturally occurring data. *Nature Computational Science*, pp. 1–12, 2024.
- Nour Makke and Sanjay Chawla. Interpretable scientific discovery with symbolic regression: a review. *Artificial Intelligence Review*, 57(1):2, 2024.
- Trent McConaghy. Ffx: Fast, scalable, deterministic symbolic regression technology. *Genetic Programming Theory and Practice IX*, pp. 235–260, 2011.
- Kazem Meidani, Parshin Shojaee, Chandan K. Reddy, and Amir Barati Farimani. SNIP: Bridging Mathematical Symbolic and Numeric Realms with Unified Pre-training. In *The Twelfth International Conference on Learning Representations*, October 2023.
- T Nathan Mundhenk, Mikel Landajuela, Ruben Glatt, Claudio P Santiago, Daniel M Faissol, and Brenden K Petersen. Symbolic regression via neural-guided genetic programming population seeding. *NeurIPS*, 2021.
- Pascal Neumann, Liwei Cao, Danilo Russo, Vassilios S Vassiliadis, and Alexei A Lapkin. A new formulation for symbolic regression to identify physico-chemical laws from experimental data. *Chemical Engineering Journal*, 387: 123412, 2020.
- Michael A Nielsen. *Neural networks and deep learning*, volume 25. Determination press San Francisco, CA, USA, 2015.
- Randal S Olson, William La Cava, Patryk Orzechowski, Ryan J Urbanowicz, and Jason H Moore. Pmlb: a large benchmark suite for machine learning evaluation and comparison. *BioData mining*, 10:1–13, 2017.
- Brenden K Petersen, Mikel Landajuela, T Nathan Mundhenk, Claudio P Santiago, Soo K Kim, and Joanne T Kim. Deep symbolic regression: Recovering mathematical expressions from data via risk-seeking policy gradients. *ICLR*, 2021.
- Markus Quade, Markus Abel, Kamran Shafi, Robert K Niven, and Bernd R Noack. Prediction of dynamical systems by symbolic regression. *Physical Review E*, 94(1):012214, 2016.
- Steven J Rigatti. Random forest. *Journal of Insurance Medicine*, 47(1):31–39, 2017.
- Cicero dos Santos, Ming Tan, Bing Xiang, and Bowen Zhou. Attentive pooling networks. *arXiv preprint arXiv:1602.03609*, 2016.
- Martin Schmelzer, Richard P Dwight, and Paola Cinnella. Discovery of algebraic reynolds-stress models using sparse symbolic regression. *Flow, Turbulence and Combustion*, 104:579–603, 2020.
- Michael D Schmidt and Hod Lipson. Age-fitness pareto optimization. In *Proceedings of the 12th annual conference on Genetic and evolutionary computation*, pp. 543–544, 2010.
- Dominic P Searson, David E Leahy, and Mark J Willis. Gptips: an open source genetic programming toolbox for multigene symbolic regression. In *Proceedings of the International multiconference of engineers and computer scientists*, volume 1, pp. 77–80. Citeseer, 2010.
- David Silver, Aja Huang, Chris J Maddison, Arthur Guez, Laurent Sifre, George Van Den Driessche, Julian Schrittwieser, Ioannis Antonoglou, Veda Panneershelvam, Marc Lanctot, et al. Mastering the game of go with deep neural networks and tree search. *nature*, 529(7587):484–489, 2016.
- David Silver, Julian Schrittwieser, Karen Simonyan, Ioannis Antonoglou, Aja Huang, Arthur Guez, Thomas Hubert, Lucas Baker, Matthew Lai, Adrian Bolton, et al. Mastering the game of go without human knowledge. *nature*, 550(7676):354–359, 2017.
- Guido F Smits and Mark Kotanchek. Pareto-front exploitation in symbolic regression. *Genetic programming theory and practice II*, pp. 283–299, 2005.
- Trevor Stephens. Gplearn: Genetic programming in python, with a scikit-learn inspired api, 2016. URL <https://github.com/trevorstephens/gplearn>. Accessed: 2024-09-26.

- Steven H Strogatz. *Nonlinear dynamics and chaos: with applications to physics, biology, chemistry, and engineering*. CRC press, 2018.
- Fangzheng Sun, Yang Liu, Jian-Xun Wang, and Hao Sun. Symbolic physics learner: Discovering governing equations via monte carlo tree search. *arXiv preprint arXiv:2205.13134*, 2022.
- Sheng Sun, Runhai Ouyang, Bochao Zhang, and Tong-Yi Zhang. Data-driven discovery of formulas by symbolic regression. *MRS Bulletin*, 44(7):559–564, 2019.
- Wassim Tenachi, Rodrigo Ibata, and Foivos I Diakogiannis. Deep symbolic regression for physics guided by units constraints: toward the automated discovery of physical laws. *The Astrophysical Journal*, 959(2):99, 2023.
- Silviu-Marian Udrescu and Max Tegmark. Ai feynman: A physics-inspired method for symbolic regression. *Science Advances*, 6(16):eaay2631, 2020.
- Silviu-Marian Udrescu, Andrew Tan, Jiahai Feng, Orisvaldo Neto, Tailin Wu, and Max Tegmark. Ai feynman 2.0: Pareto-optimal symbolic regression exploiting graph modularity. *NeurIPS*, 33:4860–4871, 2020.
- Ashish Vaswani, Noam Shazeer, Niki Parmar, Jakob Uszkoreit, Llion Jones, Aidan N. Gomez, Łukasz Kaiser, and Illia Polosukhin. Attention is all you need. In *Proceedings of the 31st International Conference on Neural Information Processing Systems*, NIPS’17, pp. 6000–6010, Red Hook, NY, USA, December 2017. Curran Associates Inc. ISBN 978-1-5108-6096-4.
- Marco Virgolin, Tanja Alderliesten, and Peter AN Bosman. Linear scaling with and within semantic backpropagation-based genetic programming for symbolic regression. In *Proceedings of the genetic and evolutionary computation conference*, pp. 1084–1092, 2019.
- Marco Virgolin, Tanja Alderliesten, Cees Witteveen, and Peter AN Bosman. Improving model-based genetic programming for symbolic regression of small expressions. *Evolutionary computation*, 29(2):211–237, 2021.
- Paul MB Vitányi. How incomputable is kolmogorov complexity? *Entropy*, 22(4):408, 2020.
- Yiqun Wang, Nicholas Wagner, and James M Rondinelli. Symbolic regression in materials science. *MRS Communications*, 9(3):793–805, 2019.
- Baicheng Weng, Zhilong Song, Rilong Zhu, Qingyu Yan, Qingde Sun, Corey G Grice, Yanfa Yan, and Wan-Jian Yin. Simple descriptor derived from symbolic regression accelerating the discovery of new perovskite catalysts. *Nature communications*, 11(1):3513, 2020.
- Yilong Xu, Yang Liu, and Hao Sun. Rsrn: Reinforcement symbolic regression machine. *ICLR*, 2024.
- Hengzhe Zhang, Aimin Zhou, Hong Qian, and Hu Zhang. Ps-tree: A piecewise symbolic regression tree. *Swarm and Evolutionary Computation*, 71:101061, 2022.
- Jinghui Zhong, Liang Feng, Wentong Cai, and Yew-Soon Ong. Multifactorial genetic programming for symbolic regression problems. *IEEE transactions on systems, man, and cybernetics: systems*, 50(11):4492–4505, 2018.

A Details of MDLformer

A.1 Model Architecture of MDLformer

The MDLformer integrates an embedder, a Transformer encoder, an attention-based pooling layer, and a multilayer perceptron (MLP) as a readout head. The embedder first pad $x \in \mathbb{R}^{N \times D}$ to $\mathbb{R}^{N \times D_{\max}}$, where $D_{\max} = 10$, then concatenate it with y to obtain $(x, y) \in \mathbb{R}^{N \times D_{\max} + 1}$. The results are tokenized to triplets of sign, mantissa, and exponent, and are then embedded to D_i -dimensional embedding space, forming the $\mathbf{E} \in \mathbb{R}^{N \times D_{\max} + 1 \times 3 \times D_i}$, where $D_i = 64$. To reduce the length of the input sequence of the Transformer encoder, we adopt an MLP with a hidden layer that maps \mathbf{E} to $\mathbf{E}' \in \mathbb{R}^{N \times D_f}$, where $D_f = 512$. Without positional encoding, \mathbf{E}' is directly fed into an 8-layer Transformer encoder with 8 heads and 512 hidden units, whose feed-forward layer has a hidden size of 2048. The output of the Transformer encoder, $\mathbf{V} \in \mathbb{R}^{N \times D_f}$, is then pooled to $\mathbf{n} \in \mathbb{R}^{D_f}$ through the attention-based pooling layer. The \mathbf{n} is then fed into the read-out MLP with a hidden layer to obtain the estimated MDL $\mathcal{M}_\Phi(x, y) \in \mathbb{R}$. We clip N to no more than $N_{\max} = 200$ at the input of MDLformer. There are 31.9 million trainable parameters in the MDLformer and 30.7 million trainable parameters in the Symbolic encoder used for the alignment training objective.

A.2 Pre-training of MDLformer

We train the MDLformer in a two-step way: First, we use the alignment loss, $\mathcal{L}_{\text{align}}$, to train the MDLformer for 100k steps. Then, we use the prediction loss, $\mathcal{L}_{\text{pred}}$, to train the MDLformer for another 30k steps. During the training, we use a batch size of 1024, which consumes CUDA memory of around 150G. We use a learning rate of 10^{-3} and the noam schedule (Vaswani et al., 2017), where the warmup step is 4000. During the training, we use a dropout rate of 0.1. Trained on a machine with 8 A100-SXM4-80GB GPUs and an AMD EPYC 7742 64-Core processor, the training lasted 41 hours, during which 131 million pairs of input data were generated.

B Details of Our SR Method

We compare three different search methods in Table 3:

Genetic Programming (GP). GP (Stephens, 2016) maintains a set of candidate formulas, called population. At the initialization step, a random generation algorithm generates initial candidates in a given number as the starting population. In the update step, there are two kinds of functionals to operate on these candidates: crossover and mutation. For the crossover, two candidates are sampled from the population, whose random subformulas are then swapped with each other to obtain the new candidates. For the mutation, a candidate is sampled from the population, whose random subformula is replaced with another formula generated by a formula generator.

Monte Carlo tree search (MCTS). MCTS (Sun et al., 2022) maintains a search tree, where each node represents a formula f_i and some numbers, including total rewards Q_i and total counts N_i . At the beginning, the search tree contains only an “empty” formula $f = \square$, where \square represents a placeholder to be filled. In the update step, the MCTS algorithm starts from the root node and uses the greedy algorithm to select a formula with the largest upper confidence interval (UCB) that is not in the search tree. Specifically, it considers all possible formulas f_i obtained by filling in a mathematical symbol into a placeholder of current formulas and selects the one with the maximal UCB

$$\text{UCB}_i = \frac{Q_i}{N_i} + \sqrt{\frac{\ln(\sum_i N_i)}{N_i}}, \quad (5)$$

where \sum_i is the sum of all possible formulas. By iteratively repeating this selection until the selected formula f_i^* is not in the search tree, MCTS finds the formula to be added to the candidate set in this round. The placeholders in this formula (if any) are filled with random formulas to create several complete formulas, whose averaged prediction errors in mean square error, R , are used to update Q_i for f_i^* and its ancestors:

$$Q_i \leftarrow Q_i + \frac{\eta^{C[f^*]}}{1 + R/\sigma_y^2}, \quad (6)$$

where $\eta = 0.999$, $C[f^*]$ that evaluates the length of f^* is used as a regular term, σ_y is the standard deviation of y .

Our Method. Based on the MCTS algorithm, our method also maintains a search tree. The difference is that each node in the tree $f_i \in \mathcal{F}_{D \times D_i}$ represents D_i subformulas in the target formula. We set the root node of the search tree as $f(x) = x \in \mathcal{F}_{D \times D}$. Starting from this, we obtain the node to be added to the search tree in each round by using the

greedy algorithm to select the f_i^* with maximal PUCT Silver et al. (2016):

$$\text{PUCT}_i = \frac{Q_i}{N_i} + c_{\text{puct}} \frac{1}{\mathcal{M}_{\Phi}(f_i(x), y)} \frac{\sqrt{\sum_i N_i}}{N_i + 1}. \quad (7)$$

where $c_{\text{puct}} = 1.41$, the index i denotes all possible formulas that can be obtained by operating an unary or binary mathematical operator on 1 or 2 operands, which can be subformulas contained in the current node, variables, or numeric constants. Apart from these, the other parts are the same as the traditional MCTS approach introduced above.

Table 3: Comparison of existing search regression methods and ours

Method	Step (Initialize, Update, Select)
GP	$\{f_i\}_{i \in \text{Population}} := \{\text{Randomly Generated } f\}$ $\{f_i\}_i \leftarrow \{f_i\}_i \cup \{\text{Cross}(f_i, f_j)\}_{i,j} \cup \{\text{Mutate}(f_i)\}_i$ $\{f_i\}_i \leftarrow \text{topk}_{f \in \{f_i\}_i} \ y - f(x)\ ^2$
MCTS	$\{f_i\}_{i \in \text{MCtree}} := \{\square\}$ $\{f_i\}_i \leftarrow \{f_i\}_i \cup \{f_i^*\}$, where f_i^* has a maximum UCB selected by a greedy algorithm
Ours	$\{f_i\}_{i \in \text{MCtree}} := \{x\}$ $\{f_i\}_i \leftarrow \{f_i\}_i \cup \{f_i^*\}$, f_i^* has a maximum PUCT selected by a greedy algorithm

C Detailed Experiment Results

C.1 Symbolic Regression

C.1.1 Baselines

In our experiments, we considered a large number of baseline methods, both the ones that come with SRbench and the most recently proposed ones, ensuring the breadth of comparison.

Search methods. The vast majority of the methods we compare are search-based algorithms. Among them, genetic programming algorithms are the primary, including GPlearn (Stephens, 2016), AFP & AFP-FE (Schmidt & Lipson, 2010), ITEA (de Franca & Aldeia, 2021), EPLEX (La Cava et al., 2016), MRGP (Arnaldo et al., 2014), SBP-GP (Virgolin et al., 2019), GP-GOMEA (Virgolin et al., 2021), and Operon (Burlacu et al., 2020). In addition to this, we also compare some recent approaches based on reinforcement learning, including SPL that leverages the Monte Carlo tree search (Sun et al., 2022), DSR that relies on the deep reinforcement learning (Petersen et al., 2021), and RSRM that uses a double Q-learning algorithm (Xu et al., 2024). Finally, recent approaches that combine multiple search methods are also compared, including AI Feynman 2.0 (Udrescu et al., 2020) and BSR (Jin et al., 2020),

Other methods. We compare a series of novel methods that leverage large-scale pre-trained Transformer-based neural networks to predict the target formulas directly, including NeurSR (Biggio et al., 2021), E2ESR (Kamienny et al., 2022), and SNIP (Meidani et al., 2023).

Regression methods. We also include a neural network-based regression method, FEAT (La Cava et al., 2019). For the experiment on the black box problem set, additional regression methods based on linear regression, MLP fitting, and Kernel Ridge model are included as well.

Decision tree methods. For the experiment on the black box problem set, we also consider the XGBoost (Chen & Guestrin, 2016), AdaBoost (Freund & Schapire, 1997), Random Forest (Rigatti, 2017), and LightGBM (Ke et al., 2017) model, which can be considered as a special type of formula with discontinuous selection operators,

C.1.2 Ground-Truth Problem Set

We provided the detailed experiment results on the ground-truth problem set in Table 4, 5, 6, and 7, finding the recovery rate of our method always outperforms other methods, while its running time is always within a reasonable range. Note that although we provide complexity in these tables, it is not that a smaller value is better, since the ground-truth formula itself has its length. We also provide the Pareto fronts balancing “recovery rate – search time” and “test R^2 – complexity” as in Figure 8, finding our method always on the rank 1 of the Pareto front.

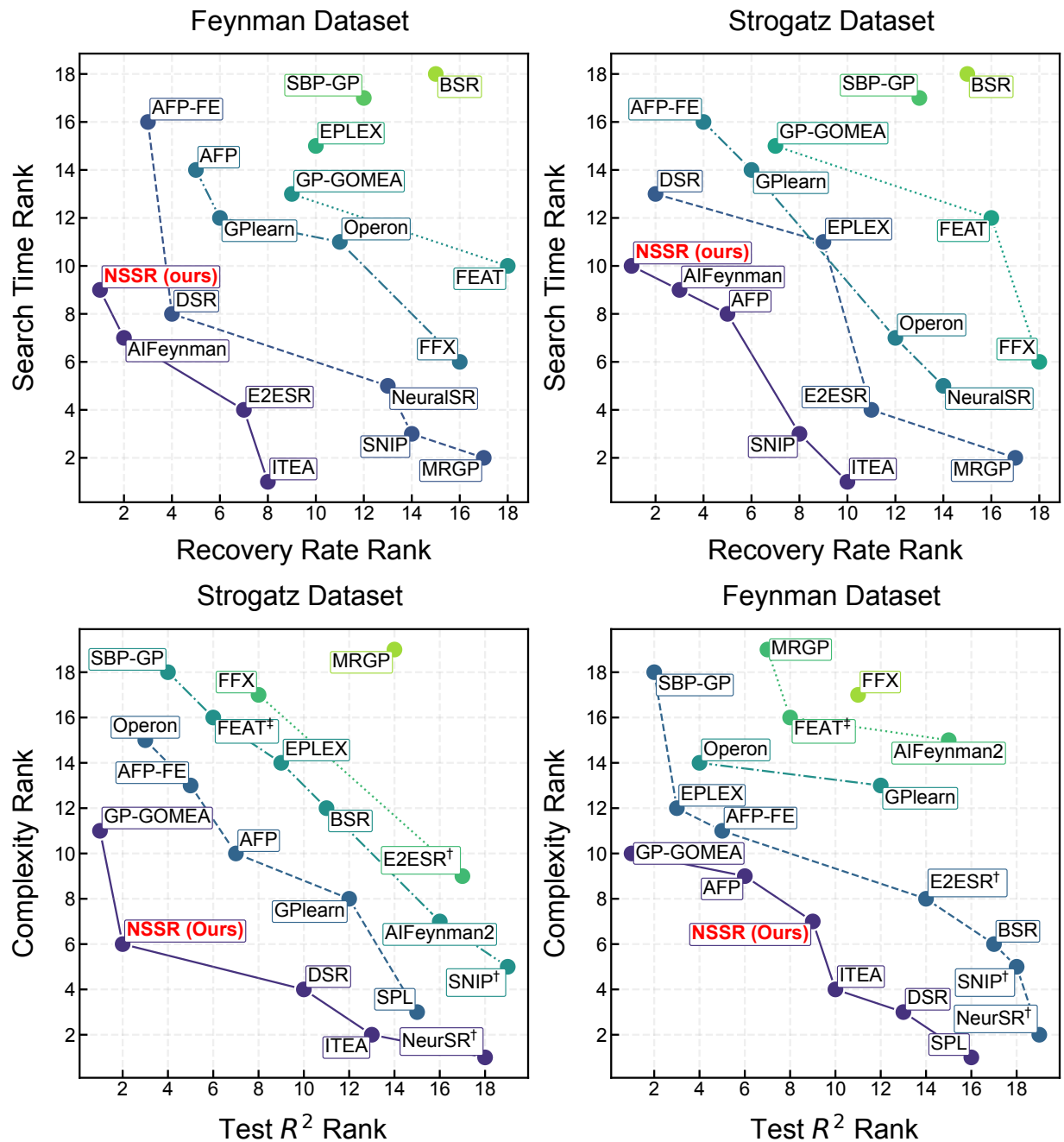


Figure 8: Pareto fronts balancing “recovery rate – search time” and “test R^2 – complexity” on Feynman and Strogatz datasets.

Table 4: **Complete experimental results at a noise level $\epsilon = 0.0$.** The results include test set R^2 , recovery rate, search time, and model size of different methods in the Feynman and Strogatz datasets, each experiment is conducted under 10 random seeds. (The same as Tables 5,6,7.)

Type	Method	Strogatz Dataset ($\epsilon = 0.0$)					Feynman Dataset ($\epsilon = 0.0$)				
		$R^2 \uparrow$	R. Rate \uparrow	Time (s) \downarrow	Complex \downarrow	$R^2 \uparrow$	R. Rate \uparrow	Time (s) \downarrow	Complex \downarrow	Time (s) \downarrow	Complex \downarrow
Regression	FEAT	0.9210(± 0.054)	0.92%($\pm 3\%$)	1135(± 970)	119(± 16)	0.9190(± 0.014)	0.00%($\pm 0\%$)	2417(± 1737)	205.3(± 13)		
Generative	NeurSR	0.5206(± 0.029)	0.00%($\pm 0\%$)	14.82(± 1.7)	11.3 (± 0.51)	0.3958(± 0.013)	3.20%($\pm 1\%$)	24.18(± 2.2)	13.28 (± 0.15)		
	E2ESR	0.5341(± 0.043)	6.06%($\pm 5\%$)	3.729(± 2)	32.49(± 2.9)	0.8570(± 0.013)	12.90%($\pm 1\%$)	4.062(± 1.3)	36.02(± 0.88)		
	SNIP	0.3995(± 0.093)	7.14%($\pm 0\%$)	1.371 (± 0.17)	16.77(± 0.59)	0.6480(± 0.037)	1.68%($\pm 1\%$)	1.901 (± 0.14)	24.87(± 0.10)		
Search	GPlearn	0.7689(± 0.067)	8.93%($\pm 3\%$)	1195(± 592)	28.96(± 2.8)	0.8809(± 0.027)	16.41%($\pm 4\%$)	3900(± 1052)	72.43(± 29)		
	AFP	0.9248(± 0.041)	15.18%($\pm 6\%$)	192.2(± 106)	38.17(± 2.8)	0.9590(± 0.005)	21.12%($\pm 2\%$)	3655(± 1999)	36.87(± 2.2)		
	AFP-FE	0.9442(± 0.045)	20.00%($\pm 11\%$)	11041(± 14277)	46.16(± 4.1)	0.9806(± 0.007)	26.98%($\pm 3\%$)	17817(± 530)	39.97(± 1.9)		
	EPLEX	0.8125(± 0.065)	8.93%($\pm 5\%$)	548.2(± 258)	50.09(± 2.7)	0.9869(± 0.006)	12.39%($\pm 2\%$)	12771(± 4998)	52.95(± 1.3)		
	SBP-GP	0.9812(± 0.016)	11.61%($\pm 5\%$)	17591(± 1765)	712.2(± 39)	0.9945(± 0.001)	12.72%($\pm 2\%$)	28901(± 37)	489.4(± 16)		
	GP-GOMEA	0.9925 (± 0.009)	29.46%($\pm 10\%$)	2760(± 1258)	36.43(± 2.4)	0.9956 (± 0.003)	26.83%($\pm 2\%$)	5030(± 967)	34.57(± 1.5)		
	Operon	0.9878(± 0.023)	11.43%($\pm 6\%$)	66.58(± 10)	59.23(± 2.1)	0.9889(± 0.006)	16.55%($\pm 4\%$)	2174(± 373)	69.88(± 1.8)		
	SPL	0.7390(± 0.047)	7.94%($\pm 2\%$)	322.1(± 180)	14.55(± 2.5)	0.7073(± 0.011)	10.37%($\pm 1\%$)	209(± 145)	12.88(± 0.57)		
	DSR	0.7602(± 0.086)	19.64%($\pm 6\%$)	1858(± 2617)	15.6(± 1.7)	0.8441(± 0.091)	19.72%($\pm 8\%$)	1733(± 3105)	14.86(± 1)		
	RSRM	0.5501(± 0.103)	4.20%($\pm 4\%$)	121.9(± 36)	13.09(± 2.3)	0.8003(± 0.013)	16.07%($\pm 2\%$)	116.3(± 31)	13.17(± 0.47)		
	AlFeynman2	0.6459(± 0.039)	28.24%($\pm 0\%$)	762.1(± 424)	22.26(± 1.7)	0.9314(± 0.016)	57.32% ($\pm 1\%$)	854.3(± 24)	124.5(± 16)		
	BSR	0.8455(± 0.044)	0.89%($\pm 3\%$)	31380(± 23952)	38.98(± 5.4)	0.6609(± 0.018)	2.48%($\pm 1\%$)	29065(± 765)	25.5(± 0.23)		
Ours		0.9900(± 0.009)	67.86% ($\pm 10\%$)	186.6(± 35)	14.07(± 1.9)	0.9171(± 0.005)	39.92%($\pm 2\%$)	467.3(± 415)	23.4(± 1.2)		
Rank		2	1	6	3	9	2	6	5		

Table 5: Complete experimental results at a noise level $\epsilon = 0.001$.

Type	Method	Strogatz Dataset ($\epsilon = 0.001$)				Feynman Dataset ($\epsilon = 0.001$)			
		$R^2 \uparrow$	R. Rate \uparrow	Time (s) \downarrow	Complex \downarrow	$R^2 \uparrow$	R. Rate \uparrow	Time (s) \downarrow	Complex \downarrow
Regression	FEAT	0.9244(± 0.032)	0.00%($\pm 0\%$)	594.4(± 181)	106.7(± 15)	0.9207(± 0.006)	0.00%($\pm 0\%$)	1726(± 242)	196.5(± 12)
	NeurSR	0.5219(± 0.031)	0.00%($\pm 0\%$)	15.07(± 1.7)	11.41 (± 0.31)	0.3979(± 0.013)	3.45%($\pm 1\%$)	24.51(± 1.7)	13.24(± 0.13)
	E2ESR	0.5105(± 0.060)	0.00%($\pm 0\%$)	3.436(± 0.75)	33.83(± 4.4)	0.8585(± 0.010)	11.46%($\pm 2\%$)	3.894(± 0.98)	35.85(± 1.5)
	SNIP	0.4220(± 0.059)	6.43%($\pm 2\%$)	1.344 (± 0.16)	16.66(± 0.65)	0.6576(± 0.025)	2.02%($\pm 1\%$)	1.926 (± 0.18)	24.88(± 0.18)
Generative	GPlearn	0.7955(± 0.067)	9.29%($\pm 3\%$)	913.3(± 121)	29.59(± 2.5)	0.8902(± 0.008)	17.27%($\pm 3\%$)	3316(± 540)	60.49(± 12)
	AFP	0.9172(± 0.052)	13.57%($\pm 7\%$)	143.4(± 27)	38.75(± 4.6)	0.9606(± 0.006)	19.66%($\pm 2\%$)	3711(± 457)	39.33(± 1.6)
	AFP-FE	0.9447(± 0.042)	15.71%($\pm 8\%$)	8108(± 584)	48.74(± 3)	0.9805(± 0.007)	21.90%($\pm 4\%$)	26160(± 157)	46.47(± 1.2)
	EPLEX	0.8488(± 0.053)	9.29%($\pm 5\%$)	416.1(± 81)	49.26(± 4.7)	0.9866(± 0.007)	9.57%($\pm 1\%$)	12341(± 436)	56.03(± 1.3)
	SBP-GP	0.9879(± 0.015)	0.00%($\pm 0\%$)	19596(± 1233)	820.5(± 41)	0.9953(± 0.001)	0.78%($\pm 1\%$)	28940(± 20)	574.4(± 13)
	GP-GOMEA	0.9914(± 0.009)	7.14%($\pm 7\%$)	804(± 603)	41.14(± 2.9)	0.9962 (± 0.001)	11.03%($\pm 2\%$)	2904(± 146)	45.23(± 0.71)
	Operon	0.9843(± 0.036)	5.00%($\pm 3\%$)	75.68(± 14)	67.03(± 5.5)	0.9916(± 0.005)	13.19%($\pm 2\%$)	2195(± 404)	69.67(± 1.6)
	SPL	0.7526(± 0.049)	7.63%($\pm 2\%$)	358.8(± 211)	14.4(± 2.5)	0.7073(± 0.016)	10.28%($\pm 2\%$)	275.5(± 206)	13.15(± 0.44)
	DSR	0.8067(± 0.048)	19.29%($\pm 3\%$)	500.8(± 317)	18.66(± 2.2)	0.8764(± 0.003)	19.14%($\pm 1\%$)	830.1(± 282)	16.04(± 0.31)
	RSRM	0.5447(± 0.105)	6.06%($\pm 6\%$)	129.7(± 8.1)	12.23(± 0.65)	0.8104(± 0.025)	17.18%($\pm 2\%$)	128.2(± 3.8)	13.04 (± 0.43)
	AI Feynman2	0.6855(± 0.091)	22.14%($\pm 5\%$)	84.19(± 74)	25.64(± 3)	0.9177(± 0.008)	33.67%($\pm 4\%$)	638(± 21)	130.6(± 17)
	BSR	0.8224(± 0.121)	0.71%($\pm 2\%$)	24299(± 3478)	37.68(± 2.2)	0.6538(± 0.023)	0.60%($\pm 1\%$)	30255(± 4770)	25.85(± 0.57)
	Ours	0.9965 (± 0.004)	73.24 %($\pm 9\%$)	171.5(± 30)	21.38(± 1.4)	0.9079(± 0.008)	34.22 %($\pm 2\%$)	428.9(± 261)	32.35(± 1.1)
	Rank	1	1	8	6	9	1	6	7

Table 6: Complete experimental results at a noise level $\epsilon = 0.01$.

Type	Method	Strogatz Dataset ($\epsilon = 0.01$)				Feynman Dataset ($\epsilon = 0.01$)			
		$R^2 \uparrow$	R. Rate \uparrow	Time (s) \downarrow	Complex \downarrow	$R^2 \uparrow$	R. Rate \uparrow	Time (s) \downarrow	Complex \downarrow
Regression	FEAT	0.9244(± 0.043)	0.00%($\pm 0\%$)	472.9(± 90)	95.61(± 16)	0.9212(± 0.010)	0.00%($\pm 0\%$)	1464(± 365)	167.1(± 6.5)
	NeurSR	0.5179(± 0.042)	6.43%($\pm 2\%$)	15.48(± 1.4)	11.63 (± 0.34)	0.3942(± 0.011)	3.11%($\pm 1\%$)	24.62(± 1.7)	13.26(± 0.12)
Generative	E2ESR	0.5031(± 0.034)	1.28%($\pm 3\%$)	3.392(± 0.72)	35.94(± 1.8)	0.8345(± 0.007)	9.72%($\pm 2\%$)	4.274(± 0.58)	40.07(± 0.90)
	SNIP	0.4562(± 0.052)	7.14%($\pm 0\%$)	1.418 (± 0.22)	18.1(± 1.3)	0.6550(± 0.029)	2.61%($\pm 2\%$)	2.19 (± 0.23)	26.96(± 0.40)
Search	GPlearn	0.7956(± 0.059)	9.29%($\pm 5\%$)	907.4(± 110)	30.59(± 4.3)	0.8890(± 0.009)	16.99%($\pm 3\%$)	3351(± 437)	60.07(± 19)
	AFP	0.9153(± 0.053)	11.43%($\pm 6\%$)	152.2(± 15)	38.62(± 7.1)	0.9610(± 0.005)	16.90%($\pm 3\%$)	4090(± 758)	40.86(± 1.1)
	AFP-FE	0.9582(± 0.041)	13.57%($\pm 8\%$)	8898(± 579)	48.8(± 5.4)	0.9819(± 0.008)	20.78%($\pm 4\%$)	27763(± 297)	46.92(± 2.3)
	EPLEX	0.8562(± 0.040)	4.29%($\pm 4\%$)	437.6(± 64)	53.07(± 3.8)	0.9910(± 0.002)	8.71%($\pm 2\%$)	11043(± 718)	54(± 0.68)
	SBP-GP	0.9813(± 0.015)	0.00%($\pm 0\%$)	20783(± 776)	850.9(± 34)	0.9950(± 0.001)	0.00%($\pm 0\%$)	28954(± 15)	595.5(± 12)
	GP-GOMEA	0.9783(± 0.029)	1.43%($\pm 3\%$)	765.6(± 1005)	42.64(± 4.5)	0.9967 (± 0.001)	5.09%($\pm 1\%$)	3020(± 360)	44.67(± 1.1)
	Operon	0.9829 (± 0.031)	0.71%($\pm 2\%$)	94.92(± 15)	81.68(± 1.2)	0.9878(± 0.010)	2.07%($\pm 1\%$)	3165(± 549)	87.96(± 1.3)
	SPL	0.7388(± 0.060)	7.91%($\pm 4\%$)	413.3(± 295)	14.71(± 1.8)	0.7133(± 0.007)	11.24%($\pm 2\%$)	295.1(± 175)	13.43(± 0.58)
	DSR	0.8199(± 0.055)	18.57%($\pm 4\%$)	492.9(± 287)	18.51(± 1.2)	0.8782(± 0.004)	18.97%($\pm 1\%$)	929.8(± 422)	16.2(± 0.41)
	RSRM	0.5969(± 0.077)	4.31%($\pm 5\%$)	142.2(± 21)	14.22(± 1.5)	0.8092(± 0.015)	15.00%($\pm 3\%$)	131.6(± 14)	12.97 (± 0.34)
	AlFeynman2	0.7753(± 0.047)	9.29%($\pm 8\%$)	85.17(± 75)	32.41(± 4.1)	0.8732(± 0.021)	13.86%($\pm 4\%$)	629.4(± 5.9)	155.2(± 8)
	BSR	0.8127(± 0.070)	0.00%($\pm 0\%$)	23622(± 554)	38.74(± 2.6)	0.6734(± 0.018)	0.09%($\pm 0\%$)	30411(± 4711)	28.03(± 0.49)
	Ours	0.9718(± 0.057)	62.86 %($\pm 6\%$)	505.1(± 34)	20.31(± 0.81)	0.9140(± 0.009)	31.97 %($\pm 2\%$)	844.3(± 561)	31.15(± 1.5)
	Rank	4	1	12	6	8	1	7	7

Table 7: Complete experimental results at a noise level $\epsilon = 0.1$.

Type	Method	Strogatz Dataset ($\epsilon = 0.1$)				Feynman Dataset ($\epsilon = 0.1$)			
		$R^2 \uparrow$	R. Rate \uparrow	Time (s) \downarrow	Complex \downarrow	$R^2 \uparrow$	R. Rate \uparrow	Time (s) \downarrow	Complex \downarrow
Regression	FEAT	0.9228(± 0.027)	0.00%($\pm 0\%$)	446.9(± 73)	84.2(± 15)	0.9195(± 0.006)	0.00%($\pm 0\%$)	777.9(± 102)	99.48(± 5.6)
	NeurSR	0.5054(± 0.058)	0.71%($\pm 2\%$)	17.47(± 1.6)	12.74 (± 0.37)	0.3823(± 0.020)	0.00%($\pm 0\%$)	25.81(± 1.7)	13.54(± 0.16)
	E2ESR	0.5152(± 0.038)	7.14%($\pm 5\%$)	5.621(± 4.9)	38.49(± 2.7)	0.7714(± 0.014)	7.01%($\pm 1\%$)	6.183(± 0.83)	44.09(± 0.61)
	SNIP	0.5536(± 0.057)	6.43%($\pm 4\%$)	1.695 (± 0.23)	22.55(± 1.2)	0.6669(± 0.020)	0.08%($\pm 0\%$)	2.768 (± 0.20)	30.8(± 0.32)
Generative	GPlearn	0.8228(± 0.052)	9.29%($\pm 3\%$)	894.6(± 108)	25.84(± 2.9)	0.8911(± 0.007)	16.80%($\pm 2\%$)	2938(± 543)	48.83(± 0.5)
	AFP	0.9110(± 0.065)	4.29%($\pm 4\%$)	161.4(± 28)	44.44(± 5.3)	0.9577(± 0.007)	13.10%($\pm 2\%$)	3886(± 341)	40.79(± 1.5)
	AFP-FE	0.9496(± 0.037)	2.14%($\pm 3\%$)	10082(± 565)	50.96(± 4)	0.9826(± 0.005)	13.53%($\pm 4\%$)	28812(± 0.51)	48.87(± 1.4)
	EPLEX	0.8822(± 0.078)	2.14%($\pm 5\%$)	405.8(± 43)	53.46(± 2.3)	0.9901(± 0.004)	10.17%($\pm 3\%$)	10283(± 532)	45.62(± 1.3)
	SBP-GP	0.9323(± 0.050)	0.00%($\pm 0\%$)	21886(± 782)	901.2(± 34)	0.9905(± 0.007)	0.00%($\pm 0\%$)	28932(± 83)	621.9(± 6.6)
	GP-GOMEA	0.9668(± 0.031)	0.00%($\pm 0\%$)	402.9(± 802)	43.71(± 2.1)	0.9957 (± 0.003)	1.64%($\pm 1\%$)	3186(± 454)	46.43(± 0.91)
	Operon	0.9380(± 0.042)	0.00%($\pm 0\%$)	97.13(± 15)	83.44(± 1.2)	0.9847(± 0.008)	0.09%($\pm 0\%$)	3090(± 330)	89.23(± 0.65)
	SPL	0.7715(± 0.044)	9.09%($\pm 3\%$)	355.3(± 59)	13.91(± 1.6)	0.7109(± 0.013)	10.00%($\pm 2\%$)	270(± 168)	13.54(± 0.50)
	DSR	0.8086(± 0.047)	15.00%($\pm 5\%$)	500(± 300)	18.51(± 2.2)	0.8779(± 0.002)	16.81%($\pm 2\%$)	814.9(± 197)	16.03(± 0.46)
	RSRM	0.5553(± 0.057)	3.81%($\pm 5\%$)	138.3(± 6.4)	13.54(± 1.1)	0.8104(± 0.016)	13.98%($\pm 2\%$)	133.8(± 6)	12.81 (± 0.41)
	AIFeynman2	0.3170(± 0.082)	2.16%($\pm 4\%$)	65.97(± 19)	23.53(± 4.6)	0.2248($\pm \text{nan}$)	0.83%($\pm \text{nan}\%$)	710.7($\pm \text{nan}$)	176.6($\pm \text{nan}$)
	BSR	0.7190(± 0.076)	0.00%($\pm 0\%$)	23292(± 510)	49.54(± 4.9)	0.6567(± 0.024)	0.00%($\pm 0\%$)	32497(± 7914)	28.77(± 1.1)
Search	Ours	0.9686 (± 0.057)	62.86 %($\pm 14\%$)	522.6(± 43)	20.5(± 0.62)	0.9097(± 0.009)	28.79 %($\pm 1\%$)	962.9(± 0.18)	30.86(± 1.4)
	Rank	1	1	13	5	8	1	9	7

C.1.3 Black-Box Problem Set

We provide the detailed result of the experiments on the black-box problem set as in Table 8, where our method achieves the rank 1 of the Pareto front within a reasonable timeframe, meaning it can balance the accuracy (measured by the test set R^2) and simplicity (i.e., formula complexity) better than other baseline methods.

Table 8: **Complete experimental results of black box dataset.**

Pareto Rank	Method	Test R^2 \uparrow	Complexity \downarrow	Time (s) \downarrow
1	Operon	0.7945	65.69	2974
	GP-GOMEA	0.7381	30.27	9636
	NSSR (Ours)	0.6258	29.88	541.7
	DSR	0.5625	9.465	36852
2	SBP-GP	0.7869	634	149344
	FEAT [‡]	0.7621	82.49	6432
	EPLEX	0.7372	53.14	15796
	AFP-FE	0.6400	36.04	6184
	AFP	0.6333	34.89	6033
	GPlearn	0.5390	19.06	24254
	Linear [‡]	0.4437	17.4	0.2447
	NeurSR [†]	0.1228	13.33	11.7
3	XGB*	0.7496	20186	236
	AdaBoost*	0.6939	9481	65.12
	LGBM*	0.6410	5734	29.9
	ITEA	0.6295	116.7	12183
	SNIP [†]	0.3335	38.91	3.286
	BSR	0.2725	22.52	59822
4	RandomForest*	0.6615	1517178	120.4
	KernelRidge [‡]	0.5952	1824	39.19
	FFX	0.5575	1562	244.3
	E2ESR [†]	0.3612	61.09	7.101
5	MRGP	0.5300	10802	165007
	MLP [‡]	0.5238	3882	30.49
	AlFeynman2	0.2110	2240	86854

C.2 Prediction Performance of MDLformer

C.2.1 Metrics

In addition to the RMSE, R^2 , and AUC metrics we provided in the main text, we also considered another three metrics as in Table 9. All metrics illustrate the excellent performance of MDLformer in estimating the value of MDL. The definitions of these metrics are provided as follows:

- **RMSE** evaluates the average difference between the prediction value and the ground truth:

$$\text{RMSE} = \sqrt{\frac{1}{K} \sum_i^K (y_i - \hat{y}_i)^2} \quad (8)$$

- **R^2** evaluates the strength of the linear relationship between the predicted value and the target value:

$$R^2 = 1 - \frac{\sum_i^K (y_i - \hat{y}_i)^2}{\sum_i^K (y_i - \bar{y})^2} \quad (9)$$

- **AUC** is a ranking metric, which evaluates the likelihood that the predicted values and the true values maintain consistent ordering when randomly selecting pairs:

$$\text{ROC} = \frac{\sum_i^K \sum_{j \neq i}^K \mathbb{I}((y_i - y_j)(\hat{y}_i - \hat{y}_j) > 0)}{K(K-1)}, \quad (10)$$

where \mathbb{I} is the indicator function.

- ρ_{Spearman} is another ranking metric, which is defined as

$$\rho_{\text{Spearman}} = 1 - \frac{6 \sum_i^K (r_i - \hat{r}_i)^2}{N(N^2 - 1)}, \quad (11)$$

where r_i is the rank of y_i , ranging from small to large, and the similar as \hat{r}_i .

- ρ_{Pearson} , or the correlation coefficient, is a widely used metric for estimating the degree of correlation between two variables, which is defined as

$$\rho_{\text{Pearson}} = \frac{\text{cov}(y, \hat{y})}{\sigma_y \sigma_{\hat{y}}} = \frac{\sum_i^K (y_i - \bar{y})(\hat{y}_i - \bar{\hat{y}})}{\sqrt{\sum_i^K (y_i - \bar{y})^2} \sqrt{\sum_i^K (\hat{y}_i - \bar{\hat{y}})^2}} \quad (12)$$

- NDCG_R is a ranking metric that is defined as

$$\text{NDCG}_R = \frac{\sum_r^R (2^{y_{i_r}} - 1) / \log_2(r + 1)}{\sum_r^R (2^{y_r} - 1) / \log_2(r + 1)}, \quad (13)$$

where y_r is the r -th smallest value in y , \hat{i}_r is the index of the r -th smallest value in \hat{y} , where we chose $R = 5$.

RMSE	R^2	AUC	ρ_{Spearman}	ρ_{Pearson}	NDCG_5
3.9105	0.9035	0.8859	0.9542	0.9506	0.7264

Table 9: **Detailed Prediction performance of MDLformer.**

C.2.2 Ablation study

We provide the AUC metric of the ablation study as in Figure 9, where we can find similar conclusions as in the main text. That is, 1) the sequential training strategy outperforms the other two strategies, 2) the performance of MDL estimation increases as the number of input samples increases, and 3) the RMSE performance decreases as the feature noise gets stronger while the AUC performance keeps robust.

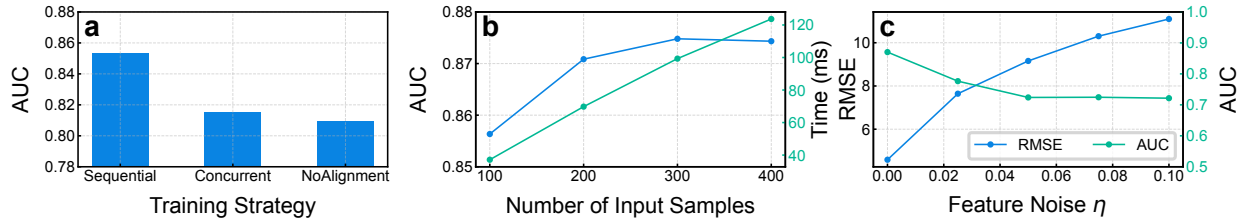


Figure 9: **AUC metric in ablation study.**